Expression, solubilization, and biochemical characterization of the tight junction transmembrane protein claudin-4

LAURA L. MITIC,[1,4] VINZENZ M. UNGER,[2] AND JAMES MELVIN ANDERSON[1,3]

[1]Department of Internal Medicine and Cell Biology, [2]Department of Molecular Biophysics and Biochemistry, Yale University School of Medicine, New Haven, Connecticut 06520, USA
[3]Department of Cell and Molecular Physiology, University of North Carolina-Chapel Hill, Chapel Hill, North Carolina 27599, USA

(RECEIVED July 2, 2002; FINAL REVISION October 18, 2002; ACCEPTED October 31, 2002)

Abstract

The tight junction tetraspan protein claudin-4 creates a charge-selective pore in the paracellular pathway across epithelia. The structure of the pore is unknown, but is presumed to result from transcellular adhesive contacts between claudin's extracellular loops. Here we report the expression of claudin-4 by baculovirus infection of Sf9 cells and describe the biochemical analysis suggesting it has a hexameric quaternary configuration. We show the detergent perfluoro-octanoic acid is able to maintain oligomeric claudin species. Sucrose velocity centrifugation and laser light scattering are also used to investigate the oligomeric state of claudin-4. In contrast to proteins of similar topology, such as gap junction family connexins, the oligomeric state of claudins appears more dynamic. These data suggest the structural organization of claudins in tight junction pores is unique.

Keywords: Claudin; tight junction; perfluoro-octanoic acid (PFO); oligomer

Claudins are a 20-member family of tetraspan membrane proteins that, together with another tetraspan protein called occludin, create the selective barrier between epithelia and endothelia called the tight junction. The tight junction was first identified ultrastructurally as several close membrane contacts at the apico-lateral end of endothelial and epithelial cells (Farquhar and Palade 1963). These focal appositions visualized by transmission electron microscopy are created by adhesive contacts among claudins and occludin. Claudins and occludin are ordered into linear polymers, termed fibrils, which encircle the apical end of the lateral cell membrane and can be visualized by freeze fracture electron microscopy (Furuse et al. 1998b). Transfection of L cells, which do not contain tight junction transmembrane proteins, with either claudin or occludin results in the de novo appearance of fibrils, although claudin fibrils are dramatically more elaborate than occludin fibrils (Furuse et al. 1998b). These fibrils are formed by lines of transmembrane particles of 10 nm diameter; when fixed with glutaraldehyde the particles fuse (Bullivant 1977). Both claudins (~23 kD) and occludin (~65 kD) have cytoplasmic N- and C-termini with two extracellular loops (Furuse et al. 1993; Furuse et al. 1998a), and extracellular adhesive loop contacts presumably create the tight junction seal. The physical structure of these contacts is unknown, although it is expected to be highly unique since the resultant pore allows selective passage of ions through the paracellular space between cells without generating a channel in the plasma membrane. Whether claudin physically interacts with occludin and

Reprint requests to: James Melvin Anderson, Department of Cell and Molecular Physiology, University of North Carolina-Chapel Hill, 266 Medical Sciences Research, Building CB# 7545, Chapel Hill, NC 27599-7545, USA; e-mail: jandersn@med.unc.edu; fax: (919) 966-6413.

[4]Present address: Department of Biochemistry and Biophysics, University of California, San Francisco, 513 Parnassus Ave., San Francisco, CA 94143-0448, USA

Abbreviations: cldn-4, claudin-4; PFO, perfluoro-octanoic acid; DDM, dodecyl maltoside; OG, β-octylglucoside; DHPC, diheptanoyl-glycerol-3-phosphocholine; DOC, sodium deoxcholate; ZW-16, zwittergent-16; LLS, laser light scattering.

Article and publication are at http://www.proteinscience.org/cgi/doi/10.1110/ps.0233903.

whether claudins can form heteromeric assemblies is also unknown. Since endogenous claudins are in low abundance in vertebrate epithelial cells, we overexpressed cldn-4 in a heterologous cell system to make available the amount necessary for biophysical characterization.

Functionally, the tight junction is a discriminating barrier, exhibiting ionic and size selectivity (for review, see Reuss 2001). Claudins are directly responsible for the charge selective movement of ions in the paracellular space (Van Itallie et al. 2001; Colegio et al. 2002). Claudin-4 overexpressed in MDCK cells creates monolayers with decreased permeability to sodium (Van Itallie et al. 2001), suggesting claudin-4 selectively restricts passage of sodium in the paracellular space. Reversing the charge of a single residue in the first extracellular loop of claudin-4 from positive to negative reverses the sodium permeability so that it is increased, suggesting charge selectivity is conferred by individual residues in the extracellular loops. Tight junctions of different organs and cell types exhibit widely varying junctional characteristics, presumably created by differing combinations of claudins. Expression profiles support this hypothesis, with distinct localization of claudins in the rat digestive tract (Rahner et al. 2001), nephron (Simon et al. 1999; Enck et al. 2001; Kiuchi-Saishin et al. 2002), testis (Gow et al. 1999), and ear (Wilcox et al. 2001). How claudins assemble in three dimensions to create this selective pore is unknown.

Comparison with other intramembrane protein particles of known composition suggest tight junction particles are composed of claudin multimers. Each particle is approximately 10 nm in diameter. 10-nm particles are also observed in freeze fracture replicas of gap junctions (Goodenough 1976) and Xenopus oocytes overexpressing a neuronal glutamate receptor (Eskandari et al. 2000). In both cases the 10-nm particle corresponds to an oligomer of membrane proteins; six connexins and five glutamate receptors, respectively. Claudins are smaller proteins (~23 kD), suggesting that 10-nm particles at the tight junction are composed of multimers of claudins. In the present study, we overexpressed claudin-4 in insect cells using the baculovirus expression system and characterized its detergent solubility and oligomerization state. Claudin-4's behavior in SDS and perfluoro-octanoic acid suggests it forms multimers. However, stable oligomeric forms were not observed in other detergents, suggesting the supramolecular organization of claudins in tight junctions varies significantly from the rigid organization of tetrapan oligomers at other types of junctions such as gap junctions.

Results

Overexpression of claudin-4 in insect cells

Claudin-4 was overexpressed in *Spodoptera frugiperda* (Sf9) or *Trichoplusia ni* (High-Five) cells by recombinant baculovirus infection. These insect cells do not contain any endogenous claudins or other tight junction proteins and provide a heterologous cell expression system in which to produce large amounts of claudin-4 free of additional complicating protein–protein interactions. Human claudin-4 cDNA was C-terminally tagged with 10 histidine residues, subcloned into pFastBac and integrated into the baculovirus genome. Recombinant virus was amplified and used to infect cells at a multiplicity of infection between 7 and 10. Immunoblots of infected whole-cell lysate or crude Sf9 membrane preparations probed with monoclonal anti-His or anti-claudin-4 antibodies revealed a single band of ~23 kD (Fig. 1), the expected molecular mass of claudin-4. This band was also visible in Coomassie-stained gels of membrane preparations (Fig. 1), demonstrating robust overexpression of this small membrane protein.

Immunocytochemistry of infected cells revealed a granular cytoplasmic distribution of claudin-4 (data not shown). Infected cells did not stick together, or otherwise show evidence of adhesive homotypic claudin interactions on the cell surface. By freeze fracture electron microscopy, we did not observe any tight-junction-like fibrils or particles as are typically found in mammalian fibroblast cells transfected with claudins (data not shown). Immuno-EM revealed that claudin-4 is concentrated in intracellular membranes, most likely those of the ER or Golgi, and does not appear on the

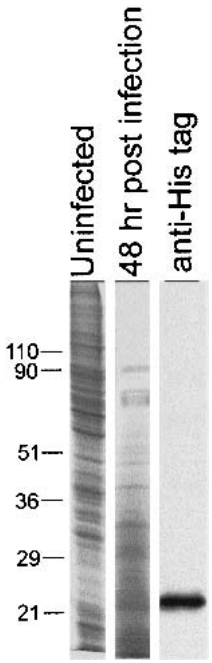

Figure 1. Human claudin-4 is robustly overexpressed in Sf9 cells using the baculovirus expression system. Coomassie brilliant blue staining of total cell lysates from uninfected (lane *1*) and infected (lane *2*) cells 48 h postinfection reveals an increase in visible proteins at ~23 kD. Immunoblotting using an antibody directed against the C-terminal histidine tag produces a band of the expected size for claudin-4 at ~23 kD (lane *3*).

plasma membrane (data not shown). Multilamellar structures, previously seen in Sf9 cells overexpressing the tight junction membrane protein occludin (Furuse et al. 1996), were not observed. Together, these data suggest that claudin-4 overexpressed in insect cells is retained inside cells and does not form the continuous chains observed in vertebrate cells.

Claudin-4 is variably solubilized by multiple detergents

To determine the solubility of claudin-4 expressed in insect cells, we exposed crude Sf9 membranes from infected cells to a panel of 39 detergents. Our choice of detergents was motivated by differences in head groups and hydrophobic regions—the 39 used cover the main classes of detergents. Identical amounts of membrane were used to compare the effectiveness of each detergent. To ensure complete solubilization, the amount of detergent used was equivalent to the mass of the dried membrane pellet plus 1 × the critical micelle concentration (CMC). Samples were agitated for 1 h at room temperature, centrifuged for 30 min at 100,000*g*, and the resultant supernatant was mixed with SDS sample buffer and loaded on a 13% SDS-PAGE gel. As visible in Figure 2, cldn-4 is variably soluble in 33 of 39 detergents. These results are quantitated in Table 1. In general, ionic and phospholipid-like detergents were most effective at liberating cldn-4 from the membrane. However, nonionic detergents solubilized only a small fraction or no percentage of cldn-4. These results identified a number of candidate detergents for further characterization and purification of cldn-4.

PFO-solubilization produces SDS-resistant adducts of cldn-4 on SDS-PAGE gels

During the detergent extraction studies, we noticed several detergents produced additional immunoreactive bands suggestive of oligomeric adducts. Multimeric bands were never more than a very small percentage of the total signal, with the striking exception of the detergent perfluoro-octanoic acid (PFO). PFO resulted in a clearly visible ladder of six bands on a 13% SDS-PAGE gel, which caused us to further characterize it hydrodynamically. In comparison to migration of soluble protein standards, the apparent molecular masses of these bands are consistent with claudin monomers (20.4 kD), dimers (41.7 kD), trimers (61.7 kD), tetramers (77.6 kD), pentamers (89.1 kD), and hexamers (107.2 kD), although resolution diminishes at the top of the gel (Fig. 3A,B). Evaluation of the same sample on an 8% gel did not reveal additional high molecular weight adducts, confirming six as the total number of visible adducts (data not shown). SDS-resistant adducts are routinely seen with other membrane proteins, such as connexins. These results suggest PFO permits maintenance of oligomeric claudin-4 species and SDS is unable to completely disrupt a complex previously exposed to PFO.

PFO-PAGE reveals a claudin-4 oligomer

To further characterize the putative oligomeric species maintained by PFO, we used the novel gel system PFO-PAGE, in which PFO is used in place of SDS in gel electrophoresis. PFO-PAGE has been previously demonstrated to maintain the native quaternary structure of membrane proteins such as aquaporin 1 and band 3 (Ramjeesingh et al. 1999), the chloride channel CIC-2 (Ramjeesingh et al. 2000), and the vanilloid receptor 1 (Kedei et al. 2001). Membranes were solubilized in 8% PFO, clarified by a 100,000*g* spin, electrophoresed in 4%–20% native gels in PFO running buffer, and probed with anti-His antibodies. Claudin-4 migrated as a broad band, ranging from ~50 to >140 kD, with most immunoreactivity concentrated at ~120 kD, which is consistent with a hexameric configuration

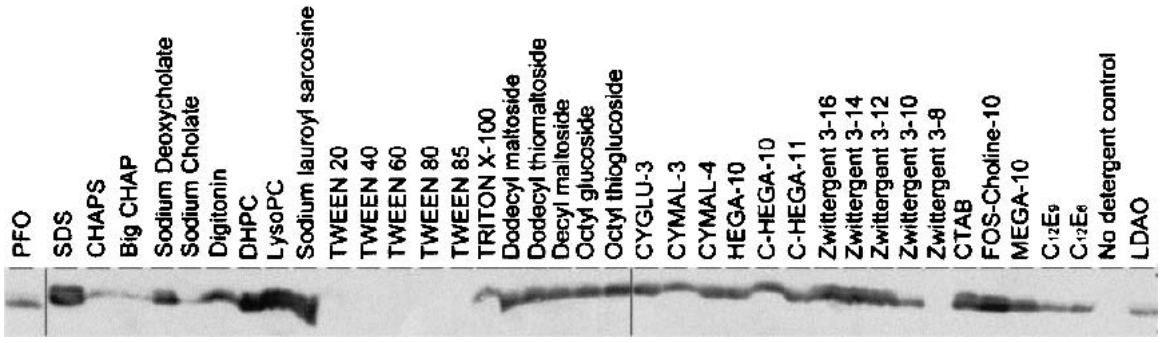

Figure 2. Extractability of claudin-4 from Sf9 cells by 39 detergents in 210 mM NaCl and 20 mM Hepes, pH 7.4. Crude membrane preparations of Sf9 cells were mixed with a quantity of freshly prepared detergent equivalent to the dry pellet mass of membranes plus the amount required to obtain 1X the CMC. Samples were incubated with stirring for 1 h at RT, spun 30 min at 100,000*g*, and soluble supernatant was mixed with 5X SDS sample buffer. Sample was electrophoresed on 13% SDS-PAGE gels and detected using anti-His antibodies. Protein solubility is quantitated in Table 1.

Table 1. *Detergent used*

	Mol. wt (Da)	CMC (mM) in water	Total protein extracted (IOD—arbitrary units)	Percent protein extracted (SDS = 100%)
Group 1				
1,2-Diheptanoyl glycero-3-phosphocholine (DHPC)	481.6	1.7	3157.3	164.6
LysoPC	495.6	1.4	2488.5	129.7
Fos-Choline-10	323.4	11.0	2295.6	119.7
Sodium lauroyl sarcosine	293.4	14.4	1974.2	102.9
Sodium Dodecyl Sulfate (SDS)	288.4	2.6	1918.1	100.0
Group II				
Zwittergent 3-14	363.6	0.4	1192.2	62.2
Cetyltrimethylammonium bromide (CTAB)	364.5	1.0	1066.7	55.6
Zwittergent 3-16	391.6	0.06	997.4	52.0
Deoxycholic acid	414.60	8.0	990.0	51.6
Digitonin	1229.3	6.0	902.4	47.1
n-Dodecyl-β-D-maltoside	510.6	0.17	856.2	44.6
Zwittergent 3-12	335.6	4.0	852.6	44.5
n-Octyl-β-D-thioglucoside	308.4	9.0	810.1	42.2
n-Dodecyl-β-D-thiomaltoside	526.6	0.05	771.5	40.2
Decanoyl-N-methylglucamide (MEGA-10)	349.5	6–7.0	699.1	36.4
n-Cyclohexyl-propyl-β-D-glucoside (CYGLU-3)	308.4	28.0	607.3	31.7
n-Octyl-β-D-glucoside (OG)	292.4	18–20.0	607.2	31.7
n-Decyl-β-D-maltoside	482.6	1.8	573.7	29.9
Perfluoro-octanoic acid (PFO)	414.07	27.5	564.6	29.4
Cyclohexyl-butyl-β-D-maltoside (CYMAL-4)	480.5	7.6	560.4	29.2
Cyclohexylpentanoyl-N-hydroethylglucamide (C-HEGA-11)	391.5	11.5	520.2	27.1
Decanoyl-N-hydroxyethylglucamide (HEGA-10)	379.5	7.0	508.7	26.5
Cyclohexylbutanoyl-N-hydroethylglucamide (C-HEGA-10)	377.5	35.0	485.9	25.3
Group III				
Cyclohexyl-propyl-β-D-maltoside (CYMAL-3)	466.5	34.5	342.2	17.8
Zwittergent 3-10	307.6	4.0	296.8	15.5
$C_{12}E_6$	451.10	0.09	263.0	13.7
TRITON X-100	631.0	0.9	241.2	12.6
$C_{12}E_9$	583.10	0.08	232.6	12.1
Sodium Cholate	430.6	15.0	185.4	9.7
Lauryldimethylamine-N-oxide (LDAO)	229.4	1–2	183.7	9.6
CHAPS	619.9	14	146.0	7.6
Gluconamidopropyl cholamide (Big CHAP)	878.1	3.4	82.6	4.3
TWEEN-20			28.1	1.5
Zwittergent 3-8	279.6	330	12.2	0.6
TWEEN-40			0	0
TWEEN-60			0	0
TWEEN-80			0	0
TWEEN-85			0	0
No detergent control	—	—	0	0

(Fig. 4A). Although bands are typically diffuse in this system because of the lack of a focusing step, the broadness of this band suggested multiple oligomeric species exist in PFO lysates. Mass was approximated based on comparison with the linear relationship between the distance of migration and the logarithm of molecular weight of soluble protein standards (Fig. 4B).

To further characterize these multiple species, we performed sucrose velocity centrifugation. High-speed PFO supernatant was loaded onto a 5%–20% sucrose gradient containing PFO and centrifuged for 8 h at 25°C at 187,813*g*, midtube (39,000 rpm). Because of the unusually high specific density of PFO (1.6), separation is achieved in only 8 h, as opposed to > 20 h for a more typical detergent whose specific density is near 1.0. Gradient fractions were electrophoresed on 13% SDS gels, again revealing a ladder of adducts, but with larger adducts shifted farther into the gradient. Specifically, monomeric and dimeric species were concentrated in fractions 7 and 8, trimers in fractions 9–11, tetramers in fractions 10 and 11, pentamers in fractions 11

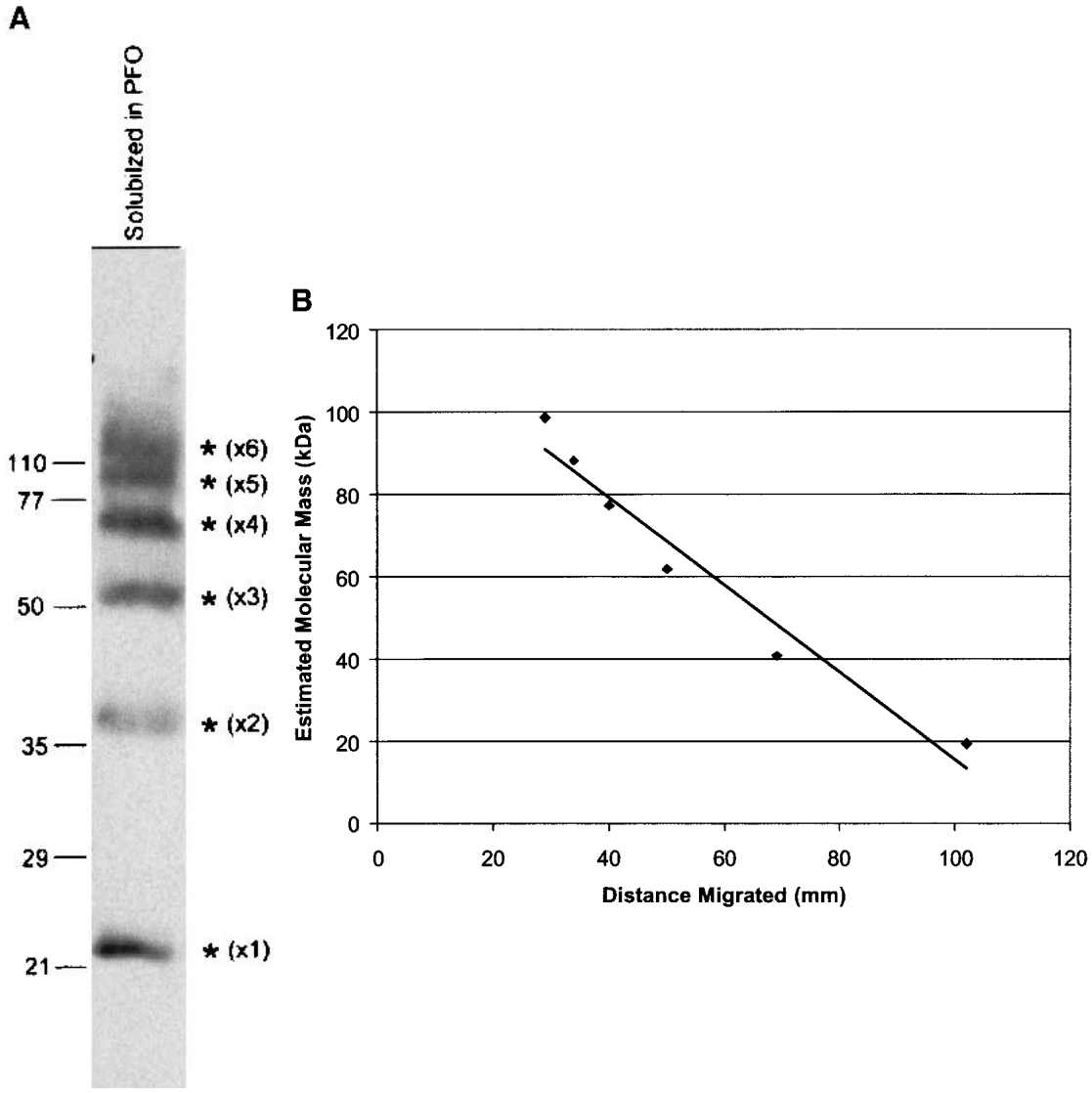

Figure 3. Visualization of claudin-4 SDS-resistant adducts. (*A*) Claudin-4 is solubilized in PFO, electrophoresed on a 13% SDS-PAGE gel, and detected using anti-His antibodies. Six immuno-reactive bands are visible (*). (*B*) A plot of the distance migrated by each band versus its expected molecular mass as extrapolated from the migration of protein standards reveals a linear relationship.

and 12, and hexamers in fraction 12 (Fig. 5). In this experiment, membranes are exposed solely to PFO before loading on the PFO-containing sucrose gradient and mixed with SDS sample buffer only after fractionation. Thus, the HMW species are not artifacts from exposure to SDS, since they migrate as discrete species before being exposed to SDS.

Identical samples were also separated by PFO-PAGE. As seen in Figure 6, samples increase in apparent molecular mass across the gradient. A PFO sucrose gradient was fractionated as in Figure 5, and samples were mixed with PFO sample buffer (instead of SDS as above) and electrophoresed on a 4%–20% PFO-PAGE gel. Estimated sizes range from ~50 kD in fraction 7 to ~120 kD in fraction 13. These data confirm PFO solubilization produces a range of oligomeric species that can be resolved by velocity gradient centrifugation.

Sucrose velocity centrifugation of claudin-4 using additional detergents suggests solubilization with DDM also maintains a putative claudin oligomer

To identify detergents that maintain the claudin oligomer without partially disrupting it as PFO does, we performed sucrose velocity centrifugation of claudin-4 membranes solubilized in a variety of nonionic and zwitterionic detergents. The specific densities of all these detergents are between 0.81 and 0.91, making possible comparisons of protein sedimentation. High-speed supernatants were loaded

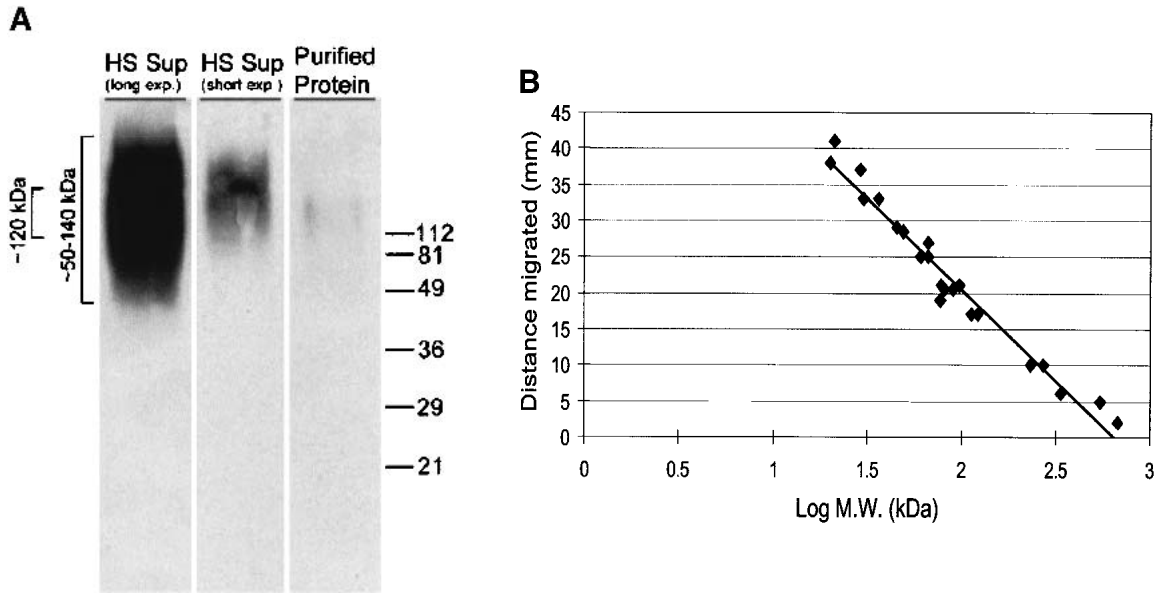

Figure 4. PFO-PAGE reveals PFO maintains claudin-4 oligomers. (*A*) Cldn-4 SF9 membranes were solubilized for 1 h at RT in PFO, spun 30 min at 100,000*g* and the resultant high speed (HS) supernatant was mixed with PFO sample buffer. Sample was loaded on 4%–20% native gels preelectrophoresed in PFO-containing running buffer. Anti-His immunoblot of HS sup (lanes *1*,*2*) or PFO-purified protein (lane *3*) reveals a range of sizes (long exposure), with the majority of protein concentrated at ~120 kD (short exposure and purified protein). (*B*) The distance migrated by soluble protein standards versus their log MW is plotted, showing a linear relationship between molecular mass and migration in the PFO-PAGE system.

onto 5%–20% sucrose gradients containing 0.1% detergent and centrifuged in a Beckman SW41 rotor at 39,000 rpm for 22 h at 4°C. As shown in Figure 7, depending on the detergent, we observed a peak near the top or middle of the gradient. Protein solubilized in β-octylglucoside (OG) or diheptanoyl-glycerol-3-phosphocholine (DHPC) sedimented with a peak centered at fraction 4 (Fig. 7). Similar results were obtained with Triton X-100, sodium deoxycholate (DOC), and zwittergent-16 (ZW-16) (data not shown). Protein solubilized by CHAPS sedimented with a peak in fraction 5 (data not shown). Based on sedimentation of soluble protein markers, the peak at fractions 4–5 likely represents a claudin monomer. In contrast, solubilization in dodecyl maltoside (DDM) produced a peak centered at fraction 8, consistent with a larger oligomeric species (Fig. 7). These sedimentation profiles suggested that DDM maintained a larger oligomeric species, while OG, DHPC, DOC, ZW-16, and CHAPS disrupted the oligomer during solubilization. However, an estimate of the approximate molecular mass of the DDM species by comparison with sedimen-

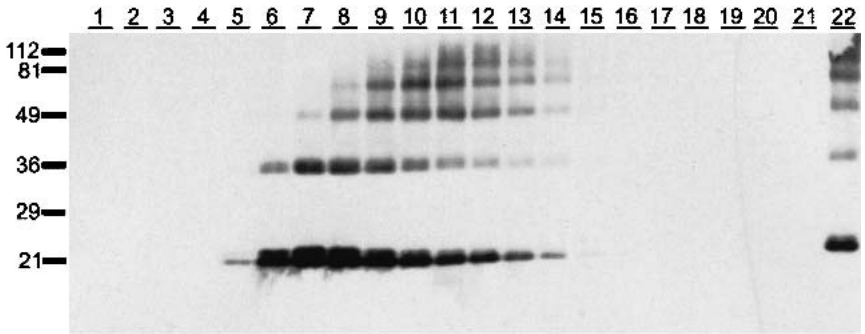

Figure 5. Cldn-4-PFO oligomeric species can be separated by sucrose velocity centrifugation. Claudin-4 was solubilized in PFO as in Figure 4 and sedimented in a 5%–20% PFO-containing sucrose gradient for 8 h at RT at 39,000 rpm in an SW41 rotor. The gradient was fractionated by hand, mixed with SDS sample buffer, loaded on a 13% SDS-PAGE gel, and detected using anti-His antibodies. Larger species migrate farther into the gradient; monomers and dimers are concentrated in fractions 7 and 8, trimers in fractions 9–11, tetramers in fractions 10 and 11, pentamers in fractions 11 and 12, and hexamers in fraction 12. Additional immunoreactivity is visible in the pellet (fraction 22).

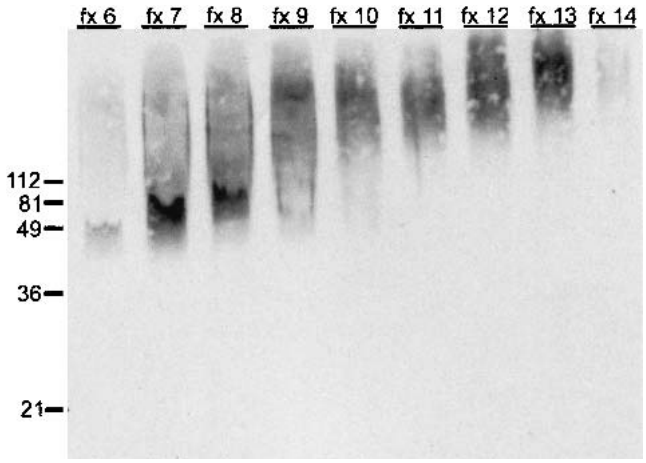

Figure 6. PFO-PAGE of sucrose gradient fractions 6–14 reveals a range of oligomeric species. PFO 5%–20% sucrose gradients were sedimented as in Figure 4 and PFO sample buffer was added to fractions. Fractions were electrophoresed on 4%–20% PFO-PAGE gels and detected with anti-His antibodies. A shift in size across the gradient is apparent, with smaller species (corresponding to monomer and dimer on SDS-PAGE gels in Fig. 5) in fx 6–8, midrange species (corresponding to trimer and tetramer) in fx 9–11, and larger species (corresponding to pentamer and hexamer) in fx 12–14.

tation of soluble protein standards is complicated by the contribution of an unknown amount of bound detergent. Therefore, to obtain the molecular mass of the DDM species, we performed high-pressure liquid chromatography together with laser light scattering–a technique that is insensitive to the bound detergent (Hayashi et al. 1989).

Gel filtration and laser light scattering (LLS) reveal monomeric claudin in both OG and DDM

Using a Ni-NTA column, His-tagged claudin-4 was purified in either DDM or OG. Based on the velocity gradient data (Fig. 7), we expected LLS would estimate the molecular mass of monomeric cldn-4 when solubilized in OG and oligomeric cldn-4 when solubilized in DDM. Protein was loaded onto a detergent equilibrated Superdex 200 gel filtration column, and UV, light scattering, and refractive index detectors analyzed eluate. Molecular mass was estimated using the three-detector method of Hayashi et al (1989), which is insensitive to the amount of bound detergent or lipid (Hayashi et al. 1989). Surprisingly, the estimated molecular mass of protein solubilized in either DDM or OG was ~23 kD, the size of monomeric claudin-4. These data suggest the shifted sedimentation profile of DDM-solubilized claudin-4 seen by sucrose velocity centrifugation represented an anomalous shift not related to oligomeric state, perhaps produced by a highly compacted conformation that contributed to a larger sedimentation value.

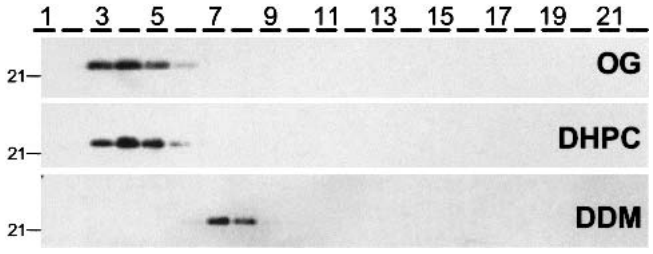

Figure 7. Sucrose velocity centrifugation of cldn-4 suggests DDM maintains a larger species than OG or DHPC. Cldn-4 Sf9 membranes were solubilized in detergent for 1 h at RT, spun 30 min at 100,000*g* and the resultant HS sup was spun through a 5%–20% sucrose gradient for 22 h at 39,000 rpm in an SW41 rotor (at 4°C). Fractions were mixed with SDS sample buffer, separated on 13% SDS-PAGE gels, and detected using anti-His antibodies. DDM-solubilized cldn-4 migrates farther into the gradient, suggesting it is a larger species.

Discussion

An emerging question in the field of tetraspan membrane proteins is how proteins with identical topology, such as connexins, tetraspanins, synaptophysin, proteolipid protein, occludin, and claudins can engage in such diverse functions while using the same primary structure template. In the case of claudin and connexins, freeze fracture studies suggest both proteins assemble into 10-nm particles. However, since connexins form a communicating channel through the membrane while claudins form a pore in the extracellular space, these two proteins must form oligomers with very different quaternary structure. To work towards understanding the structure of the paracellular pore, we have taken a stepwise approach to characterizing the in vitro properties of claudin-4, beginning with its overexpression in insect cells and biochemical characterization. In the present study we show that histidine-tagged human claudin-4 can be overexpressed and purified in large quantity from baculovirus-infected insect cells. This provides a starting point for obtaining large quantities of protein needed for structural studies. Claudin-4 embedded in insect cell membranes is soluble in a variety of detergents, thereby revealing multiple candidate detergents for use in subsequent structural studies. Using PFO-PAGE and sucrose velocity centrifugation, we provide evidence that claudin-4 oligomers are maintained during solubilization in PFO. These data are consistent with the 10-nm size of claudin-containing tight junction fibril particles long observed by freeze fracture electron microscopy. No other detergent tested maintained claudin-4's oligomeric state, as determined by sucrose velocity centrifugation and laser light scattering, suggesting that PFO's oligomer-maintaining properties are unique. We interpret these results as evidence for the oligomeric assembly of claudin-4 in Sf9 cells. Further, our studies are consistent with a dynamic tight junction oligomer, as discussed below.

We expressed claudin in insect cells because traditional biochemical and biophysical studies of endogenous claudin-4 in epithelial cells are complicated by its interactions with multiple endogenous cytoplasmic binding partners. Claudins interact with the PDZ-containing proteins ZO-1, ZO-2, ZO-3 (Itoh et al. 1999), MUPP1 (Hamazaki et al. 2002), and PATJ (Roh et al. 2002). Further, it is not known whether claudin interacts with occludin, another fibril-forming transmembrane protein. A detergent that maintains claudin's oligomeric interactions would also likely maintain claudin's interactions with other proteins. The contributions of these additional proteins to claudin's sedimentation in sucrose velocity gradients or migration in native gels would complicate any possible interpretation. Since insect cells do not make tight junctions, expression in these cells should obviate these concerns.

However, the relevance of our observations in this heterologous cell system to claudin-4's assembly under native conditions in vertebrate epithelial cells depends on the assumption that claudin-4's oligomerization state in Sf9 cells mimics its native state. It is possible our inability to find a conventional detergent that maintains an oligomer reflects a limitation in the expression system. For instance, incorrect lipid composition, a missing unknown stabilization cofactor, or a requirement for transcellular contact may bias our results towards the monomer. Thus, it is possible that claudin-4 may readily assume a multimeric configuration stable in a variety of detergents when in its native epithelial cell environment. However, other oligomeric membrane proteins, such as connexin 32 (Stauffer et al. 1991) and the Shaker voltage-gated K^+ channel (Li et al. 1994), adopt their native quaternary structures when expressed in Sf9 cells. This suggests our results are not a general failure of membrane proteins to form stable oligomers in these cells. Moreover, our PFO results argue that an oligomeric claudin state does exist in Sf9 cells. Specifically, the migration of claudin-4 centered at 120 kD on a 4%–20% PFO gel is consistent with a hexameric claudin confirmation. In addition, six SDS-resistant claudin-4 bands are visible on SDS gels of PFO-solubilized membranes, which is also consistent with a hexamer. There is no evidence that PFO artifactually creates oligomers (Ramjeesingh et al. 1999), suggesting these data represent in vivo oligomers.

The ability of all conventional detergents tested to disrupt the claudin oligomer suggests a highly dynamic and unstable configuration. This is in contrast to other oligomers, such as connexons, which require harsh conditions to disrupt. Why would a claudin oligomer be so labile in the membrane? Evidence exists suggesting this might reflect unique in vivo properties of claudins. First, rapid massive assembly of fibrils occurs under various conditions that induce cellular stress, presumably as a protective mechanism (Kachar and Pinto da Silva 1981; Lynch et al. 1995). Kachar and Da Silva (1981) reported the emergence of tight junction strands along the entire length of lateral membranes from excised rat prostate tissue incubated at 37°C at the earliest time point tested (3 min). Similarly, Lynch et al. (1995) reported the appearance of aberrant fibrils extending laterally from tight junctions within 5 min after basolateral exposure of monolayers to protease. These examples of rapid fibril proliferation support a model where a preexisting pool of fibril components can rapidly reorganize to create functional tight junction fibrils. These data indicate the fibrils themselves are dynamic structures, and allow the speculation that their components may in turn be equally dynamic.

Additional support for dynamic oligomers comes from the paradoxical relationship between transepithelial electrical resistance (TER) and flux. Experimental manipulations that increase TER, an instantaneous measurement of ion movement through tight junctions, could be expected to decrease flux, which measures the passage of larger molecules through the junction over a longer time course (min). In other words, as the junction becomes electrically tighter, the movement of larger uncharged molecules should be retarded. However, the opposite is seen. Overexpression of occludin (Balda et al. 1996; McCarthy et al. 1996) and claudin (McCarthy et al. 2000; Van Itallie et al. 2001) increases fibril number and TER while reducing or not affecting flux. Movement of ions through claudin pores is directly dependent on the charged residues in the extracellular loops of claudins (Colegio et al. 2002). It is difficult to envision an aqueous pore with ion selectivity that can also accommodate large uncharged molecules. Thus, it has been proposed that uncharged molecules pass though transient breaks in fibrils (for review, see Mitic and Anderson 1998). Dynamic claudin oligomers may promote this proposed strand breakage and reformation, thereby enabling the uncoupling of TER and flux.

Our studies describe the robust expression of claudin-4 in insect cells and its biochemical characteristics, which will be helpful in future structural studies. Determining the structure of the claudin pore is of fundamental importance in understanding epithelial barrier function. These data provide a useful starting point for future structural approaches that will ultimately provide invaluable insight into the paracellular pathway.

Materials and methods

Cells and antibodies

Sf9 and High-Five BTI-TN-5B1–4 cells were a gift from Michael Koelle (Yale University). Sf9 cells were grown at 27°C in Sf-900 II medium (Gibco BRL) supplemented with 7% FBS and 50 U/mL penicillin/streptomycin. High-Five cells were grown at 27°C in Express Five medium (Gibco BRL) supplemented with 7% FBS and 50 U/mL penicillin/streptomycin. Mouse antipenta His

(QIAGEN) and mouse anticlaudin-4 (Zymed) were routinely used for immunoblotting at a 1:4000 dilution.

Recombinant baculovirus construction and infection

The human claudin-4 cDNA (Van Itallie et al. 2001) was PCR-amplified and decahistidine tagged using primers 5′-CGGGATC-CCTGACAATGGCCTCCATGGGGCTAC-3′ (sense) and 5′-GCTTAATGATGATGATGATGATGATGATGATGATGCTTG TCTGTGCGGGGTGGACA-3′(antisense). The resultant amplicon was shuttled through pCR2.1-Topo (Invitrogen) and subcloned into pFastBac1 (Gibco BRL). Generation of recombinant virus using the Bac-to-Bac baculovirus expression system (Gibco BRL) was according to manufacturer's instructions. First-generation virus was amplified, clarified by low-speed centrifugation, and stored at 4°C. Sf9 or High-Five cells were infected in suspension at a MOI of 7–10, incubated for 52–56 h and harvested by centrifugation.

Insect cell membrane preparations

An infected cell pellet from a 3 L culture (~25 mL) was washed 2× with 500 mL ice-cold PBS, resuspended in 75 mL ice-cold 20 mM Hepes, pH 7.4, 5 mM EDTA, 1 mM PMSF plus a 10 μg/mL protease inhibitor cocktail (leupeptin, antipain, aprotinin, and trypsin-chymotrypsin inhibitor in 10 mM Hepes, pH 7.4, Sigma) and incubated on ice for 10 min. Cells were sonicated on ice 5× for 15 sec each at power level 6, duty cycle 3 (Branson Sonifier 250). Light microscopy revealed 100% of cells were disrupted under these conditions. Cell membranes were pelleted by centrifugation for 90 min at 39,000 rpm at 4°C in a SW41 rotor (Beckmann). Peripheral membrane proteins were extracted by resuspending this pellet in 75 mL of ice-cold high-salt wash (20 mM Hepes, pH 7.4, 5 mM EDTA, 1 mM PMSF plus protease inhibitor cocktail and 300 mM NaCl), followed by sonication and centrifugation as before. Pelleted membranes were resuspended in 50 mL of either 20 mM Hepes, pH 7.4, 10 mM NaCl for detergent extraction studies, or Ni-NTA lysis buffer (50 mM NaH_2PO_4, 300 mM NaCl, and 10 mM imidazole, pH 8.0) for protein purification. Membrane droplets were snap frozen directly in liquid N_2, collected into 50 mL tubes and stored at −80°C.

Detergent extraction

100 μL aliquots of infected membranes were mixed 1:1 (v/v) with freshly prepared detergent equivalent to the mass of 100 μL dried membranes plus 1× the critical micelle concentration. Detergents were obtained from Anatrace or Avanti Polar Lipids. Extraction was performed in 20 mM Hepes, pH 7.4 containing either 10 mM NaCl ("low salt" extraction) or 210 mM NaCl ("high salt" extraction). Samples were stirred using a magnetic "flea" stir bar for 1 h at room temperature, spun 30 min at 100,000*g* at room temperature in a Beckman TLA-100 rotor, and the supernatant containing solubilized claudin-4 was removed. Supernatant was mixed with 5× SDS loading buffer and loaded onto 13% SDS-PAGE gels.

PFO-PAGE

PFO-PAGE was performed using the method described by Ramjeesingh et al. (1999). Briefly, 4%–20% native gradient gels (Jule Biotechnologies or Bio-Rad) were preelectrophoresed in PFO-running buffer (25 mM Tris base, 192 mM glycine, 0.5% (w/v) PFO (Aldrich), pH of buffer 8.0) (Ramjeesingh et al. 1999) for 45 min at 50 volts. Samples in PFO sample buffer (100 mM Tris base, 8% (w/v) PFO, 20% (v/v) glycerol, 0.005% bromophenol blue) were loaded on preelectrophoresed gels and electrophoresed at room temperature at 60–100 volts until the dye front had run off the gel. The migration of ~25 μg of each protein standard (thyroglobulin, catalase, apo-transferrin, urease, and albumin, all from Sigma) was analyzed by Coomassie Brilliant Blue staining. The migration of cldn-4 was analyzed by immunoblotting. Gels were transferred at 4°C in buffer containing 25 mM Tris, 192 mM glycine and 20% (v/v) methanol.

Sucrose velocity gradient centrifugation

Sucrose velocity centrifugation was performed using the method described by Blount and Merlie (Blount and Merlie 1988). 0.2 mL high speed supernatant from solubilzation was loaded on a 5%–20% linear sucrose gradient prepared in 20 mM Hepes and 150 mM NaCl plus 0.1% of the appropriate detergent. Gradients were formed using a Gradient Master (BioComp Instruments). Non-PFO samples were centrifuged in a Beckman SW41 rotor at 39,000 rpm for 22 h at 4°C. PFO samples were centrifuged in a Beckman SW41 rotor at 39,000 rpm for 8 h at 23°C. 0.5 mL fractions were collected by hand from the top. A portion of each fraction was mixed with sample buffer and analyzed by SDS-PAGE.

Purification of cldn-4 in OG and DDM

Sf9 membranes (5 mL per purification, from a 50 mL membrane stock obtained from a 3 L culture) were diluted 1:5 (v/v) with Ni-NTA lysis buffer (50 mM NaH_2PO_4, 300 mM NaCl, and 10 mM immidazole, pH 8.0) plus 4% detergent (w/v) and solubilized with stirring for 1 h at room temperature. Insoluble material was pelleted by 100,000*g* centrifugation for 90 min in a Beckmann SW41 rotor. The resultant high-speed supernatant was mixed with washed Ni-NTA Agarose or Superflow resin (QIAGEN) for 1 h at RT. Cldn-4 bound resin was transferred to a column and washed by gravity flow with 5 column volumes of wash buffer (50 mM NaH_2PO_4, 300 mM NaCl, 1% detergent (w/v) and 20 mM immidazole, pH 8.0). Protein was eluted by gravity flow across eight 1 mL fractions using 50 mM NaH_2PO_4, 300 mM NaCl, 1% detergent (w/v), and 250 mM immidazole, pH 8.0. An aliquot of each fraction was electrophoresed on a 13% SDS-PAGE gel and analyzed by Coomassie Brilliant Blue staining and immunoblotting. Purified protein was stored at 4°C overnight until use.

Purification of Cldn-4 in PFO

Protein was purified as above except using the following buffers: lysis buffer, pH 8.0 (25 mM NaH_2PO_4, 200 mM NaCl, 4% (w/v) PFO), wash buffer, pH 7.8 (20 mM NaH_2PO_4, 200 mM NaCl, 2% (w/v) PFO), and elution buffer, pH 6.5 (20 mM NaH_2PO_4, 150 mM NaCl, 42 mM PFO). In addition, solubilization and all purification steps were performed at 30°C to maintain PFO in solution. Centrifugation was performed at room temperature. Purified protein was stored at room temperature overnight until use.

Size exclusion chromatography and laser light scattering

Purified claudin-4 was dialyzed overnight against column buffer containing the appropriate detergent. Approximately 100 μg of

sample was loaded onto a detergent-equilibrated Superdex 200 gel filtration column, and UV, light scattering, and refractive index were recorded as the sample came off the column. Estimated molecular mass was calculated using the method of Hayashi et al. (1989).

Acknowledgments

We thank all members of the Anderson and Unger laboratories for experimental suggestions, particularly Drs. Carville Bevans, Christina Van Itallie, and Thomas Marlovits; Dr. Daniel Chase (Yale University) for help establishing baculovirus-infected insect cultures; Dr. Daniel Biemsdorfer (Yale University) for use of the Gradient Master; and Dr. Ewa Folta-Stogniew (Yale University) for HPLC/LLS experiments. This research was supported by NIH grants DK45134 (JMA), T32 DK007356 to the Section of Digestive Diseases, and core facilities grant P50 DK34989 to the Yale Liver Center.

The publication costs of this article were defrayed in part by payment of page charges. This article must therefore be hereby marked "advertisement" in accordance with 18 USC section 1734 solely to indicate this fact.

References

Balda, M.S., Whitney, J.A., Flores, C., Gonzalez, S., Cereijido, M., and Matter, K. 1996. Functional dissociation of paracellular permeability and transepithelial electrical resistance and disruption of the apical-basolateral intramembrane diffusion barrier by expression of a mutant tight junction membrane protein. *J. Cell. Biol.* **134:** 1031–1049.

Blount, P. and Merlie, J.P. 1988. Native folding of an acetylcholine receptor α subunit expressed in the absence of other receptor subunits. *J. Biol. Chem.* **263:** 1072–1080.

Bullivant, S. 1977. Evaluation of membrane structure facts and artifacts produced during freeze-fracturing. *J. Microsc.* **111:** 101–116.

Colegio, O.R., Van Itallie, C., McCrea, H., Rahner, C., and Anderson, J.M. 2002. Claudins create charge-selective channels in the paracellular pathway between epithelial cells. *Am. J. Physiol. Cell Physiol.* **283:** C142-C147.

Enck, A.H., Berger, U.V., and Yu, A.S. 2001. Claudin-2 is selectively expressed in proximal nephron in mouse kidney. *Am. J. Physiol. Renal Physiol.* **281:** F966-F974.

Eskandari, S., Kreman, M., Kavanaugh, M.P., Wright, E.M., and Zampighi, G.A. 2000. Pentameric assembly of a neuronal glutamate transporter. *Proc. Natl. Acad. Sci.* **97:** 8641–8646.

Farquhar, M.G. and Palade, G.E. 1963. Junctional complexes in various epithelia. *J. Cell. Biol.* **17:** 375–412.

Furuse, M., Hirase, T., Itoh, M., Nagafuchi, A., Yonemura, S., and Tsukita, S. 1993. Occludin: A novel integral membrane protein localizing at tight junctions. *J. Cell. Biol.* **123:** 1777–1788.

Furuse, M., Fujimoto, K., Sato, N., Hirase, T., and Tsukita, S. 1996. Overexpression of occludin, a tight junction-associated integral membrane protein, induces the formation of intracellular multilamellar bodies bearing tight junction-like structures. *J. Cell Sci.* **109:** 429–435.

Furuse, M., Fujita, K., Hiiragi, T., Fujimoto, K., and Tsukita, S. 1998a. Claudin-1 and -2: Novel integral membrane proteins localizing at tight junctions with no sequence similarity to occludin. *J. Cell. Biol.* **141:** 1539–1550.

Furuse, M., Sasaki, H., Fujimoto, K., and Tsukita, S. 1998b. A single gene product, claudin-1 or -2, reconstitutes tight junction strands and recruits occludin in fibroblasts. *J. Cell. Biol.* **143:** 391–401.

Goodenough, D.A. 1976. In vitro formation of gap junction vesicles. *J. Cell. Biol.* **68:** 220–231.

Gow, A., Southwood, C.M., Li, J.S., Pariali, M., Riordan, G.P., Brodie, S.E., Danias, J., Bronstein, J.M., Kachar, B., and Lazzarini, R.A. 1999. CNS myelin and sertoli cell tight junction strands are absent in Osp/claudin-11 null mice. *Cell* **99:** 649–659.

Hamazaki, Y., Itoh, M., Sasaki, H., Furuse, M., and Tsukita, S. 2002. Multi-PDZ domain protein 1 (MUPP1) is concentrated at tight junctions through its possible interaction with claudin-1 and junctional adhesion molecule. *J. Biol. Chem.* **277:** 455–461.

Hayashi, Y., Matsui, H., and Takagi, T. 1989. Membrane protein molecular weight determined by low-angle laser light-scattering photometry coupled with high-performance gel chromatography. *Methods Enzymol.* **172:** 514–528.

Itoh, M., Furuse, M., Morita, K., Kubota, K., Saitou, M., and Tsukita, S. 1999. Direct binding of three tight junction-associated MAGUKs, ZO-1, ZO-2, and ZO-3, with the COOH termini of claudins. *J. Cell. Biol.* **147:** 1351–1363.

Kachar, B. and Pinto da Silva, P. 1981. Rapid massive assembly of tight junction strands. *Science* **213:** 541–544.

Kedei, N., Szabo, T., Lile, J.D., Treanor, J.J., Olah, Z., Iadarola, M.J., and Blumberg, P.M. 2001. Analysis of the native quaternary structure of vanilloid receptor 1. *J. Biol. Chem.* **276:** 28613–28619.

Kiuchi-Saishin, Y., Gotoh, S., Furuse, M., Takasuga, A., Tano, Y., and Tsukita, S. 2002. Differential expression patterns of claudins, tight junction membrane proteins, in mouse nephron segments. *J. Am. Soc. Nephrol.* **13:** 875–886.

Li, M., Unwin, N., Stauffer, K.A., Jan, Y.N., and Jan, L.Y. 1994. Images of purified Shaker potassium channels. *Curr. Biol.* **4:** 110–115.

Lynch, R.D., Tkachuk-Ross, L.J., McCormack, J.M., McCarthy, K.M., Rogers, R.A., and Schneeberger, E.E. 1995. Basolateral but not apical application of protease results in a rapid rise of transepithelial electrical resistance and formation of aberrant tight junction strands in MDCK cells. *Eur J. Cell. Biol.* **66:** 257–267.

McCarthy, K.M., Skare, I.B., Stankewich, M.C., Furuse, M., Tsukita, S., Rogers, R.A., Lynch, R.D., and Schneeberger, E.E. 1996. Occludin is a functional component of the tight junction. *J. Cell Sci.* **109:** 2287–2298.

McCarthy, K.M., Francis, S.A., McCormack, J.M., Lai, J., Rogers, R.A., Skare, I.B., Lynch, R.D., and Schneeberger, E.E. 2000. Inducible expression of claudin-1-myc but not occludin-VSV-G results in aberrant tight junction strand formation in MDCK cells. *J. Cell Sci.* **113:** 3387–3398.

Mitic, L.L. and Anderson, J.M. 1998. Molecular architecture of tight junctions. *Annu. Rev. Physiol.* **60:** 121–142.

Rahner, C., Mitic, L.L., and Anderson, J.M. 2001. Heterogeneity in expression and subcellular localization of claudins 2, 3, 4, and 5 in the rat liver, pancreas, and gut. *Gastroenterology* **120:** 411–422.

Ramjeesingh, M., Huan, L.J., Garami, E., and Bear, C.E. 1999. Novel method for evaluation of the oligomeric structure of membrane proteins. *Biochem. J.* **342:** 119–123.

Ramjeesingh, M., Li, C., Huan, L.J., Garami, E., Wang, Y., and Bear, C.E. 2000. Quaternary structure of the chloride channel ClC-2. *Biochemistry* **39:** 13838–13847.

Reuss, L. 2001. Tight junction permeability to ions and water. In *Tight junctions*, 2nd ed. (eds. M. Cereijido and J.M. Anderson), pp. 61–88. CRC Press, Boca Raton, FL.

Roh, M.H., Liu, C.J., Laurinec, S., and Margolis, B. 2002. The carboxy-terminus of Zona Occludens-3 binds and recruits a mammalian homologue of discs lost to tight junctions. *J. Biol. Chem.* **20:** 20.

Simon, D.B., Lu, Y., Choate, K.A., Velazquez, H., Al-Sabban, E., Praga, M., Casari, G., Bettinelli, A., Colussi, G., Rodriguez-Soriano, J., et al. 1999. Paracellin-1, a renal tight junction protein required for paracellular Mg2+ resorption. *Science* **285:** 103–106.

Stauffer, K.A., Kumar, N.M., Gilula, N.B., and Unwin, N. 1991. Isolation and purification of gap junction channels. *J. Cell. Biol.* **115:** 141–150.

Van Itallie, C., Rahner, C., and Anderson, J.M. 2001. Regulated expression of claudin-4 decreases paracellular conductance through a selective decrease in sodium permeability. *J. Clin. Invest.* **107:** 1319–1327.

Wilcox, E.R., Burton, Q.L., Naz, S., Riazuddin, S., Smith, T.N., Ploplis, B., Belyantseva, I., Ben-Yosef, T., Liburd, N.A., Morell, R.J., et al. 2001. Mutations in the gene encoding tight junction claudin-14 cause autosomal recessive deafness DFNB29. *Cell* **104:** 165–172.